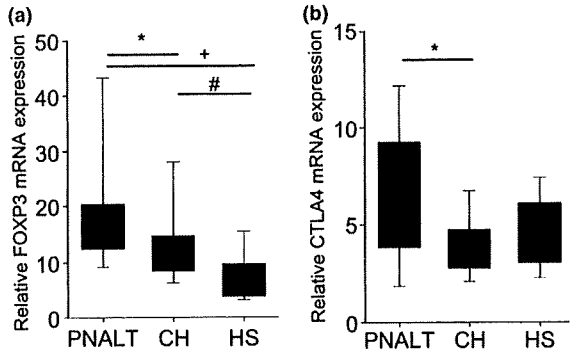

Fig. 2 Comparison of mRNA expression of FOXP3 and CTLA4 in CD4+CD25high+ T cells among the groups. The expression of FOXP3 (a) and CTLA4 (b) in separated CD4+CD25high+ T cells were analysed by real-time reverse transcriptase-polymerase chain reaction as described in Materials and methods. Boxes represent lower and upper quartiles with the median value (solid line) between boxes, while the whiskers represent the minimum and maximum values. *, $P < 0.05$; , $P < 0.01$; +, $P < 0.001$. For definitions of PNALT, CH and HS, see Fig. 1.

production stimulated with antigen-pulsed DC. We compared such responses between samples with or without CD4+CD25+ T cells. In PNALT patients, HCV NS5-specific T cell proliferation or IFN-γ production of CD25-depleted CD4+ T cells was significantly higher than those of the bulk CD4+ T cells (Fig. 3a,b). In contrast, in CH patients, such restoration did not occur significantly even when CD4+ CD25+ T cells had been depleted (Fig. 3a,b). There was no difference in the production of IL-10 and TGF-β between bulk CD4+ T cells and CD25-depleted CD4+ T cells in both CH and PNALT patients (Fig. 3c,d). These results suggest that co-existing CD4+CD25+ T cells play an inhibitory role in the HCV-specific CD4+ T cell response, in which suppression was more potent in the PNALT than in the CH group.

CD127–FOXP3+ cells, regardless of their CD25 expression, are increased in patients with HCV infection

In the analyses of N-Treg, the frequency of CD4+CD25–FOXP3+ T cells in HCV-infected patients was higher than those in the healthy donors (Fig. 1d). These results suggest that CD4+FOXP3+ T cells, regardless of the degree of CD25

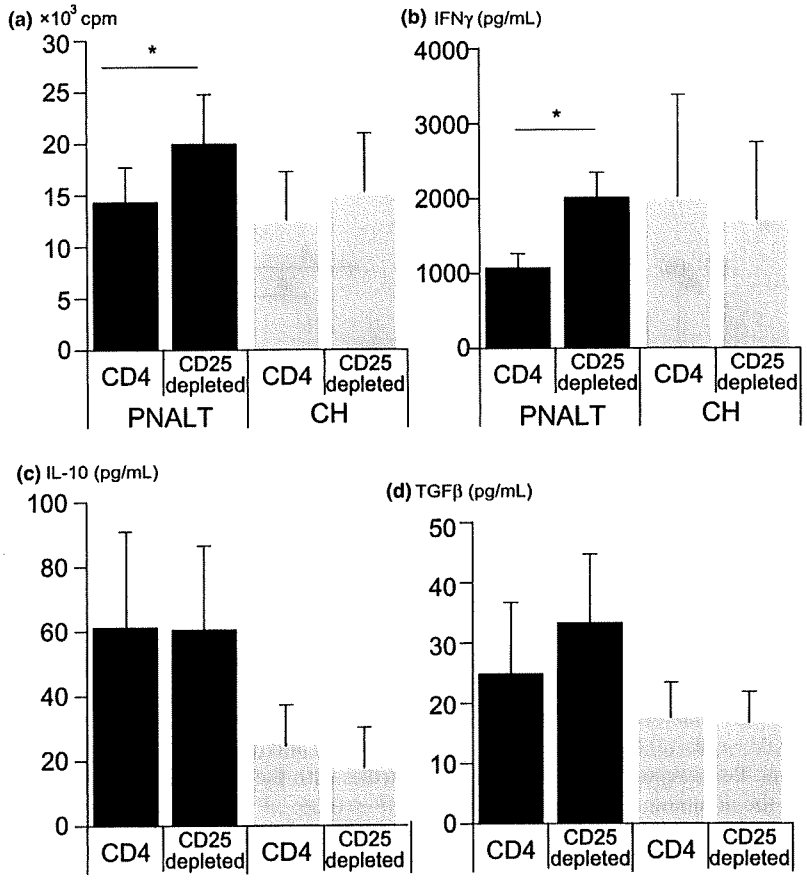

Fig. 3 Changes of hepatitis C virus (HCV)-specific CD4+ T cell responses with or without depletion of CD25+ T cells. Bulk CD4+ T cells or those depleted of CD25+ cells were cultured with autologous monocyte-derived dendritic cells in the presence of HCV-NS5 protein for 5 days as described in Materials and methods. (a) On day 4, [3H]-thymidine was pulsed and the thymidine incorporation was counted with a β-counter. Before the pulsing, the culture supernatants were harvested and subjected to enzyme-linked immunosorbent assay for interferon-γ (b), interleukin-10 (c) and TGF-β (d), respectively. *, $P < 0.05$ by Mann–Whitney *U*-test. For definitions of PNALT and CH, see Fig. 1.

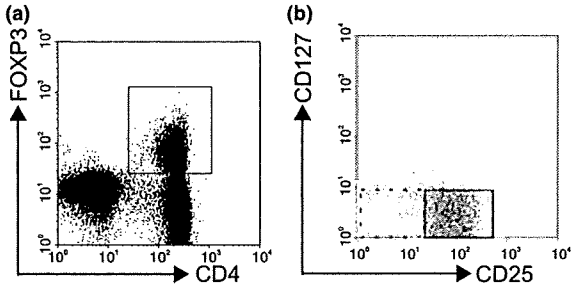

Fig. 4 Gating of CD4+CD127–FOXP3+ cells with variable CD25 expression under FACS analysis. After setting the gate on CD4+FOXP3+ cells [rectangle in the dot plot (a)], were displayed on the CD25 and CD127 axis (b). The presence of CD25+ (bold rectangle) and of CD25– cells (dotted rectangle) in CD4+FOXP3+ cells are shown in plot (b). The frequencies of these cells were analysed.

expression, increase in chronic HCV infection. Alternatively, it implies that higher expression of CD25 is not a universal marker for identifying FOXP3+ cells with regulatory activity. It has been reported that CD127 expression on CD4+ T cells is inversely correlated with FOXP3 expression, suggesting that CD127low/negative cells consist of those with regulatory activity. In order to analyse regulatory T cell subsets more precisely, we first examined FOXP3 expression on CD127– or CD127+ cells paired with CD25 expression in patients with HCV infection (Fig. 4). As a result, the majority of CD4+FOXP3+ T cells belonged to the CD127– population irrespective of CD25 expression (Fig. 4). Next, we compared the frequency of CD4+CD127–FOXP3+ cells, which consist of CD25+ and CD25– cells, among the subject groups (Fig. 5a). The frequency of CD4+CD127–FOXP3+ cells was similar in the CH and the PNALT groups, both of which were significantly higher than those in the HS (Fig. 5a). Finally, in order to estimate the profile of CD4+CD127–FOXP3+ cells according to CD25 expression, we compared the percentage of CD25+CD127–FOXP3+ or CD25–CD127–FOXP3+ cells in CD4+ T cells among the groups. The percentage of CD25+CD127–FOXP3+ T cells in CD4+ T cells was comparable for PNALT and CH (Fig. 5b). In clear contrast, the percentage of CD25–CD127–FOXP3+ T cells in the PNALT was lower than those in the CH (Fig. 5c). The frequencies of these cells were higher in the HCV-infected patients than in HS (Fig. 5b,c). When we set the focus on the proportion of CD25+CD127– or CD25-CD127– cells in the FOXP3+ cells in the periphery as a whole, we found that the proportion of CD25+CD127– cells in the PNALT was higher than that in the CH group (Fig. 5d). On the other hand, the proportion of CD25–CD127– cells in FOXP3+ cells was lower in the PNALT than in the CH group (Fig. 5e). Therefore, the phenotypic profiles of FOXP3+ T cells are distinct between PNALT and CH patients, with regard to the expression of CD127 and CD25.

DISCUSSION

Approximately 30–40% of chronically HCV-infected patients continue to display PNALT for decades. We previously reported the possible contribution of certain human leukocyte antigen haplotypes [23] or DC dysfunction in the maintenance of the PNALT state [24]. However, the precise mechanisms behind this important issue are yet to be

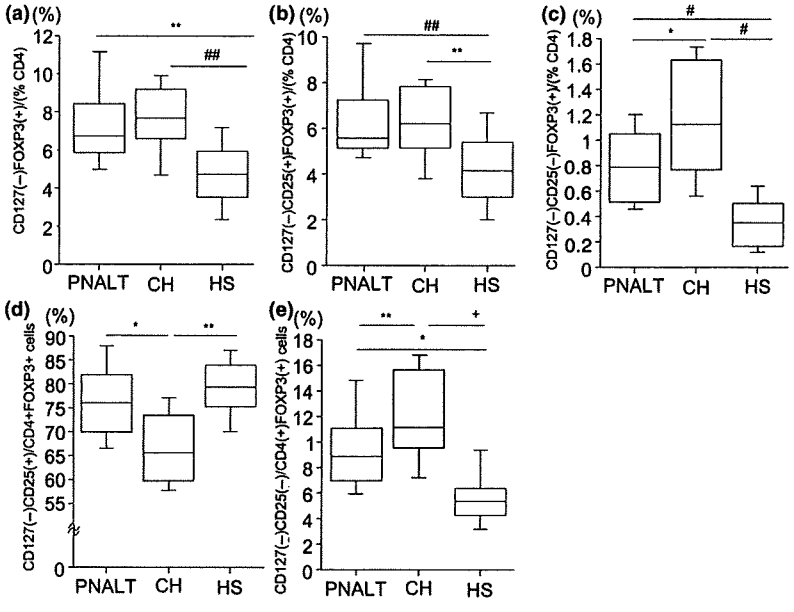

Fig. 5 Comparison in the frequencies of CD127– regulatory T cell subsets among the groups. Frequencies of CD127–FOXP3+ (a), CD127–CD25+FOXP3 (b) and CD127–CD25–FOXP3+ (c) cells among CD4+ T cells were determined by FACS analysis. The proportion of CD127–CD25+ (d) or CD127–CD25– (e) cells in CD4+FOXP3+ cells were also determined. Boxes represent lower and upper quartiles with the median value (solid line) between boxes, while the whiskers represent the minimum and maximum values. *, $P < 0.05$; , $P < 0.01$; **, $P < 0.005$; ##, $P < 0.001$; +, $P < 0.0001$ by Mann–Whitney *U*-test. For definitions of PNALT, CH and HS, see Fig. 1.

established. Cumulative reports have shown that Th1/Tc1 type responses are instrumental in HCV-induced liver inflammation [7,25,26]. We thus hypothesized that some suppressor mechanisms exist in PNALT patients especially against HCV-specific Th1 and/or CTL reactions.

The involvement of Treg cells in the pathogenesis of various diseases has been reported [9–13]. Most of the studies presented the possibility that N-Treg play substantial roles in the induction of tolerance against aetiological self or nonself antigens, thus leading to alleviation or exacerbation of the disease severity. With regard to HCV infection, several groups have shown that N-Treg are increased both in the periphery and in the liver and are able to inhibit HCV-specific CD4+ or CD8+ T cell responses *in vitro* [17,18,27]. In this study, we showed that the frequency of N-Treg in HCV-infected patients is higher than those in the controls, which is consistent with the previous reports. However, the frequencies of N-Treg are indistinguishable between the patient groups with different disease activities. As for the functional aspect, the deprivation of CD4+CD25+ cells enhanced the HCV NS5-specific CD4+ T cell response in the PNALT than in the CH group, suggesting that co-existing Treg in the PNALT are more suppressive. In addition, the expression of FOXP3 and CTLA4, which are key molecules of the suppressor function, is higher in PNALT than in those with active hepatitis. Venken *et al.* [28] demonstrated that the degree of FOXP3 expression at the single-cell level of N-Treg is well correlated with their suppressive ability, which is supportive of our results. In contrast, Bolacchi *et al.* [29] reported that the frequency of TGF-β+ N-Treg in the PNALT was higher than in the hepatitis group. Furthermore, their frequency was inversely correlated with the histological inflammatory grade, suggesting that TGF-β+ Treg play active roles in alleviating hepatitis. The reasons for the lack of correlation between N-Treg and serum ALT or HCV RNA quantity in the present study may be because of the difference in the target of analyses, such as either peripheral or intra-hepatic Treg, or either TGF-β+ or bulk Treg. Further analyses need to be performed on these important issues, as CD4+FOXP3+ Treg are reported to accumulate more in the portal tract of HCV-infected livers compared with those in the periphery [20].

During the observation period, about 30–40% of PNALT patients began to show elevated or fluctuating ALT abnormalities. What crucial factor triggers HCV-induced liver inflammation remains unknown. One of the plausible explanations is an antigenic shift accompanied by the occurrence of mutations in the HCV genome. In other words, hepatitis may flare up if the mutation raises HCV immunogenicity. Comprehensive analyses of HCV epitopes for CTL using overlapping peptides have shown that the HCV core and NS3 are more immunogenic than the remaining regions; however, the presence of an epitope hierarchy in Treg induction has been controversial. Li *et al.* [30] reported the possibility that Treg are expandable in response to certain epitopes in HCV proteins. In two patients in whom we observed flare-up of hepatitis in this study, we were able to find that the expression of FOXP3 in N-Treg was high in the PNALT status, but declined in the active hepatitis stage (data not shown). Although it is difficult to state whether such phenotypic changes in N-Treg are the cause or the consequence of disease progression, these results suggest the involvement of N-Treg in the degree of HCV-mediated hepatitis. Further detailed study is needed to examine whether or not such changes in N-Treg are related to the sequence evolution in HCV genomes.

Recent research has disclosed that distinct types of Treg are present in humans. Currently, it is generally accepted that CD25+FOXP3+ is the most reliable marker for Treg, which is induced in parallel with the acquisition of suppressor ability. However, owing to the lack of phenotypic markers for specifically identifying adaptive Treg, their roles in clinical settings have been unclear. In this study, CD4+FOXP3+ cells increased in HCV-infected patients, who were either positive or negative for CD25. In contrast to thymus-derived N-Treg expressing a greater degree of CD25, adaptive Treg are presumed to be induced in the periphery with a lesser degree of CD25 expression. Thus, it is likely that CD4+CD25–FOXP3+ T cells in HCV infection contain some part of adaptive Treg.

Treg have been reported to express low levels of CD127 at their cell surface [31]. Furthermore, the expression of CD127 is inversely correlated with FOXP3 expression and with the suppressive function of CD25high+ Treg. Liu *et al.* [22] pointed out the possibility that adaptive Treg are grouped into CD127– cells, which also include FOXP3-negative Tr1 or Th3 cells. Alternatively, You *et al.* [32] reported that murine CD4+CD25lowFOXP3+ T cells might be adaptive Treg, which exert a TGFβ-dependent suppressive function. Taking these reports into consideration, and in order to exclude activated CD25+ T cells, we examined CD4+ CD127–CD25–FOXP3+ cells tentatively determined as part of adaptive Treg. In order to confirm that CD4+CD127– cells possess suppressive capacity, we co-cultured sorted CD4+CD127–CD25– or CD4+CD127–CD25+ cells with allogeneic CD4+ T cells stimulated with anti-CD3 and anti-CD28 antibodies. As a result, we found that CD4+CD127– cells, regardless of CD25 expression, significantly suppressed the proliferation of responder CD4+ T cells (manuscript in preparation). Of note is the finding that the frequency of CD127–CD25–FOXP3+ cells is higher in patients with active hepatitis than those in the PNALT group. One of the plausible explanations for such an increase of Treg is the compensatory mechanisms for the aggravation of liver inflammation. In support of this possibility, Bonelli *et al.* [33] reported that CD4+CD127–CD25– cells are increased in patients with systemic lupus erythematosus (SLE), the numbers of which are well correlated with disease activity. With regard to the ability of Treg in SLE patients, CD4+CD127–CD25– cells were potent in the inhibition of T

cell proliferation but not in IFN-γ release. Such a defective suppressor capacity may result in the continuation of tissue inflammation regardless of the presence of abundant Treg. The other conceivable role of CD4+CD25–CD127–FOXP3+ cells in active hepatitis may be a peripheral reservoir of CD4+CD25+FOXP3+ cells in case of flare-up of liver inflammation. In mice, it has been reported that CD25–FOXP3+ cells revert to CD25+FOXP3+ cells upon activation signals, thus leading to the expansion of the Treg pool [34]. In order to reach a definite conclusion on the role of CD127–CD25–FOXP3+ cells, further analyses are needed to elucidate whether these cells are inhibitory to either HCV-specific or HCV-nonspecific T cell responses.

Large-scale studies with HCV-infected patients demonstrated that the cumulative incidence of HCC in the PNALT group is extremely low compared with that in patients with apparent hepatitis and liver cirrhosis [35]. The lesser HCC incidence is also evident in patients who attained a lasting biochemical response to IFN-based therapy; even if they had failed to achieve sustained virological response [36]. These results clearly indicate that the maintenance of the PNALT state is one of the surrogate therapeutic goals in chronic HCV infection. Therefore, it is necessary to clarify the mechanisms of Treg induction in HCV infection, whether they are naturally or adaptively introduced, and to establish a feasible modality for controlling Treg. Our study has shown the importance of subset-oriented analyses of Treg for gaining access to that goal.

ACKNOWLEDGEMENT

This study was funded in part by Ministry of Education, Culture, Sports, Science and Technology, Ministry of Health, Labor and Welfare of Japan.

CONFLICT OF INTEREST

All of the authors do not have any commercial or other association that might pose a conflict of interest.

REFERENCES

1 Kasahara A, Hayashi N, Mochizuki K *et al.* Risk factors for hepatocellular carcinoma and its incidence after interferon treatment in patients with chronic hepatitis C. Osaka Liver Disease Study Group. *Hepatology* 1998; 27(5): 1394–1402.
2 Marcellin P, Levy S, Erlinger S. Therapy of hepatitis C: patients with normal aminotransferase levels. *Hepatology* 1997; 26 (3 Suppl. 1): 133S–136S.
3 Tassopoulos NC. Treatment of patients with chronic hepatitis C and normal ALT levels. *J Hepatol* 1999; 31 (Suppl. 1): 193–196.
4 Persico M, Persico E, Suozzo R *et al.* Natural history of hepatitis C virus carriers with persistently normal aminotransferase levels. *Gastroenterology* 2000; 118(4): 760–764.
5 Suruki R, Hayashi K, Kusumoto K *et al.* Alanine aminotransferase level as a predictor of hepatitis C virus-associated hepatocellular carcinoma incidence in a community-based population in Japan. *Int J Cancer* 2006; 119(1): 192–195.
6 Nelson DR, Marousis CG, Davis GL *et al.* The role of hepatitis C virus-specific cytotoxic T lymphocytes in chronic hepatitis C. *J Immunol* 1997; 158(3): 1473–1481.
7 Schirren CA, Jung MC, Gerlach JT *et al.* Liver-derived hepatitis C virus (HCV)-specific CD4(+) T cells recognize multiple HCV epitopes and produce interferon gamma. *Hepatology* 2000; 32(3): 597–603.
8 Sakaguchi S. Naturally arising CD4+ regulatory T cells for immunologic self-tolerance and negative control of immune responses. *Annu Rev Immunol* 2004; 22: 531–562.
9 Viglietta V, Baecher-Allan C, Weiner HL, Hafler DA. Loss of functional suppression by CD4+CD25+ regulatory T cells in patients with multiple sclerosis. *J Exp Med* 2004; 199(7): 971–979.
10 Ehrenstein MR, Evans JG, Singh A *et al.* Compromised function of regulatory T cells in rheumatoid arthritis and reversal by anti-TNFalpha therapy. *J Exp Med* 2004; 200(3): 277–285.
11 Sugiyama H, Gyulai R, Toichi E *et al.* Dysfunctional blood and target tissue CD4+CD25high regulatory T cells in psoriasis: mechanism underlying unrestrained pathogenic effector T cell proliferation. *J Immunol* 2005; 174(1): 164–173.
12 Weiss L, Donkova-Petrini V, Caccavelli L, Balbo M, Carbonneil C, Levy Y. Human immunodeficiency virus-driven expansion of CD4+CD25+ regulatory T cells, which suppress HIV-specific CD4 T-cell responses in HIV-infected patients. *Blood* 2004; 104(10): 3249–3256.
13 Ormandy LA, Hillemann T, Wedemeyer H, Manns MP, Greten TF, Korangy F. Increased populations of regulatory T cells in peripheral blood of patients with hepatocellular carcinoma. *Cancer Res* 2005; 65(6): 2457–2464.
14 Jonuleit H, Schmitt E. The regulatory T cell family: distinct subsets and their interrelations. *J Immunol* 2003; 171(12): 6323–6327.
15 Hori S, Nomura T, Sakaguchi S. Control of regulatory T cell development by the transcription factor Foxp3. *Science* 2003; 299(5609): 1057–1061.
16 Fontenot JD, Rudensky AY. A well adapted regulatory contrivance: regulatory T cell development and the forkhead family transcription factor Foxp3. *Nat Immunol* 2005; 6(4): 331–337.
17 Cabrera R, Tu Z, Xu Y *et al.* An immunomodulatory role for CD4(+)CD25(+) regulatory T lymphocytes in hepatitis C virus infection. *Hepatology* 2004; 40(5): 1062–1071.
18 Rushbrook SM, Ward SM, Unitt E *et al.* Regulatory T cells suppress *in vitro* proliferation of virus-specific CD8+ T cells during persistent hepatitis C virus infection. *J Virol* 2005; 79(12): 7852–7859.
19 Sugimoto K, Ikeda F, Stadanlick J, Nunes FA, Alter HJ, Chang KM. Suppression of HCV-specific T cells without differential hierarchy demonstrated *ex vivo* in persistent HCV infection. *Hepatology* 2003; 38(6): 1437–1448.
20 Ward SM, Fox BC, Brown PJ *et al.* Quantification and localisation of FOXP3+ T lymphocytes and relation to

hepatic inflammation during chronic HCV infection. *J Hepatol* 2007; 47(3): 316–324.
21 Chen W, Jin W, Hardegen N *et al.* Conversion of peripheral CD4+CD25– naive T cells to CD4+CD25+ regulatory T cells by TGF-beta induction of transcription factor Foxp3. *J Exp Med* 2003; 198(12): 1875–1886.
22 Liu W, Putnam AL, Xu-Yu Z *et al.* CD127 expression inversely correlates with FoxP3 and suppressive function of human CD4+ Treg cells. *J Exp Med* 2006; 203(7): 1701–1711.
23 Kuzushita N, Hayashi N, Moribe T *et al.* Influence of HLA haplotypes on the clinical courses of individuals infected with hepatitis C virus. *Hepatology* 1998; 27(1): 240–244.
24 Kanto T, Inoue M, Miyazaki M *et al.* Impaired function of dendritic cells circulating in patients infected with hepatitis C virus who have persistently normal alanine aminotransferase levels. *Intervirology* 2006; 49(1–2): 58–63.
25 Leroy V, Vigan I, Mosnier JF *et al.* Phenotypic and functional characterization of intrahepatic T lymphocytes during chronic hepatitis C. *Hepatology* 2003; 38(4): 829–841.
26 Penna A, Missale G, Lamonaca V *et al.* Intrahepatic and circulating HLA class II-restricted, hepatitis C virus-specific T cells: functional characterization in patients with chronic hepatitis C. *Hepatology* 2002; 35(5): 1225–1236.
27 Boettler T, Spangenberg HC, Neumann-Haefelin C *et al.* T cells with a CD4+CD25+ regulatory phenotype suppress *in vitro* proliferation of virus-specific CD8+ T cells during chronic hepatitis C virus infection. *J Virol* 2005; 79(12): 7860–7867.
28 Venken K, Hellings N, Thewissen M *et al.* Compromised CD4+ CD25(high) regulatory T-cell function in patients with relapsing-remitting multiple sclerosis is correlated with a reduced frequency of FOXP3-positive cells and reduced FOXP3 expression at the single-cell level. *Immunology* 2008; 123(1): 79–89.
29 Bolacchi F, Sinistro A, Ciaprini C *et al.* Increased hepatitis C virus (HCV)-specific CD4+CD25+ regulatory T lymphocytes and reduced HCV-specific CD4+ T cell response in HCV-infected patients with normal versus abnormal alanine aminotransferase levels. *Clin Exp Immunol* 2006; 144(2): 188–196.
30 Li S, Jones KL, Woollard DJ *et al.* Defining target antigens for CD25+ FOXP3+ IFN-gamma-regulatory T cells in chronic hepatitis C virus infection. *Immunol Cell Biol* 2007; 85(3): 197–204.
31 Seddiki N, Santner-Nanan B, Martinson J *et al.* Expression of interleukin (IL)-2 and IL-7 receptors discriminates between human regulatory and activated T cells. *J Exp Med* 2006; 203(7): 1693–1700.
32 You S, Leforban B, Garcia C, Bach JF, Bluestone JA, Chatenoud L. Adaptive TGF-beta-dependent regulatory T cells control autoimmune diabetes and are a privileged target of anti-CD3 antibody treatment. *Proc Natl Acad Sci USA* 2007; 104(15): 6335–6340.
33 Bonelli M, Savitskaya A, Steiner CW, Rath E, Smolen JS, Scheinecker C. Phenotypic and functional analysis of CD4+CD25– Foxp3+ T cells in patients with systemic lupus erythematosus. *J Immunol* 2009; 182(3): 1689–1695.
34 Zelenay S, Lopes-Carvalho T, Caramalho I, Moraes-Fontes MF, Rebelo M, Demengeot J. Foxp3+ CD25– CD4 T cells constitute a reservoir of committed regulatory cells that regain CD25 expression upon homeostatic expansion. *Proc Natl Acad Sci USA* 2005; 102(11): 4091–4096.
35 Okanoue T, Makiyama A, Nakayama M *et al.* A follow-up study to determine the value of liver biopsy and need for antiviral therapy for hepatitis C virus carriers with persistently normal serum aminotransferase. *J Hepatol* 2005; 43(4): 599–605.
36 Tanaka H, Tsukuma H, Kasahara A *et al.* Effect of interferon therapy on the incidence of hepatocellular carcinoma and mortality of patients with chronic hepatitis C: a retrospective cohort study of 738 patients. *Int J Cancer* 2000; 87(5): 741–749.

J Gastroenterol (2009) 44:834–841
DOI 10.1007/s00535-009-0077-z

ORIGINAL ARTICLE—ALIMENTARY TRACT

Restoration of gut motility in Kit-deficient mice by bone marrow transplantation

Shuji Ishii · Shingo Tsuji · Masahiko Tsujii · Tsutomu Nishida · Kenji Watabe · Hideki Iijima · Tetsuo Takehara · Sunao Kawano · Norio Hayashi

Received: 29 January 2009 / Accepted: 2 April 2009 / Published online: 21 May 2009

Abstract
Purpose Interstitial cells of Cajal (ICC) play important roles in autonomic gut motility as electrical pacemakers and mediators of neural regulation of smooth muscle functions. Insufficiency of ICC has been reported in a wide range of gut dysmotilities. Thus, restoration of ICC may be a therapeutic modality in these diseases. Here we provide evidence that transplanted bone marrow (BM) cells can restore gut dysmotility in part via transdifferentiation to ICC.
Methods Bone marrow cells obtained from Kit insufficient *W/W^v* mice or syngeneic GFP-transgenic mice with wild-type *Kit* were transferred to *W/W^v* recipients. Whole gut transit time and gastric emptying were examined 5 and 6 weeks after BM transplantation, respectively, and ICCs were identified in whole mounts, frozen sections and transmission electron immunomicroscopy of the gut smooth muscle layers using specific antibodies.
Results Transplantation of wild-type BM into *W/W^v* mice significantly improved whole gut transit time and gastric emptying. Fluorescent immunohistochemistry revealed GFP$^+$Kit$^+$ cells in the myenteric plexus, deep muscular plexus, and submucosal plexus smooth muscle layers of the stomach, small intestine, and colon, respectively. In the whole mounts, GFP$^+$Kit$^+$ cells were bipolar and spindle shaped, and transmission electron immunomicroscopy showed GFP$^+$ cells rich in mitochondria and endoplasmic reticulum between gut smooth muscle layers, suggesting the presence of GFP$^+$ cells with morphological characteristics of ICC.
Conclusions These results suggest that BM contains cells that may incorporate into ICC networks and improve dysmotility in *W/W^v* mice. Thus, BM transplantation may become to a new therapeutic modality for gut dysmotilities due to ICC insufficiency.

Keywords Bone marrow · Green fluorescent protein · Interstitial cells of Cajal

Abbreviations

BM	Bone marrow
ICC	Interstitial cells of Cajal
GFP	Green fluorescent protein
FBS	Fetal bovine serum
PBS	Phosphate buffered saline
AIC	Anti-ICC antibody
DAPI	4′, 6-Diamino-2-phenylindole

Introduction

Rhythmic contractile activity of gastrointestinal smooth muscles is driven by electrical signals (slow waves) generated by interstitial cells of Cajal (ICC) [1]. ICC may also

S. Ishii (✉) · S. Tsuji · M. Tsujii · T. Nishida · K. Watabe · H. Iijima · T. Takehara · N. Hayashi
Department of Gastroenterology and Hepatology (K1), Osaka University Graduate School of Medicine, 2-2 Yamadaoka, Suita, Osaka 565-0871, Japan
e-mail: sishii@gh.med.osaka-u.ac.jp

S. Kawano
Department of Clinical Laboratory Science, Osaka University Graduate School of Medicine, 2-2 Yamadaoka, Suita, Osaka 565-0871, Japan

Present Address:
S. Kawano
Rinku General Medical Center, Izumisano Hospital, Izumisano, Osaka 598-8577, Japan

play similar roles in other tubular, smooth muscle-lined organs, such as the urethra and lymph vessels, in a wide range of species [2]. Absence of, or a decrease in, ICC has been reported in patients with chronic pseudo-obstruction [3], achalasia of cardia [4], pyloric stenosis [4], colonic inertia [5], afferent loop syndrome [6], internal anal sphincter achalasia [7], Hirschsprung's disease [7], and gut dysmotility associated with diabetes mellitus [8–10]. In addition, partial bowel obstruction [11], surgical resection of the gut [12], and jejunal inflammation [13] disrupt ICC networks and cause abnormal motility. Patients suffering from these disorders would likely benefit from the restoration of ICC. However, the developmental origin of ICC remains unclear [14]. Although tissue precursors for gastric ICC have recently been identified [15], these cells are rare and not yet available for cellular therapy. Bone marrow (BM) is an alternative source of multipotent stem cells that can distribute into various organs and may transdifferentiate into various cells, including hepatocytes [16], skeletal muscle fibers [17], cardiomyocytes [18], and gastrointestinal epithelial cells [19]. We previously reported that BM-derived cells can transdifferentiate into both epithelial and stromal cells of the colon [20] and stomach [21] in rats.

Kit, a receptor tyrosine kinase, plays an important role in ICC development. Blocking Kit function may cause ICC transdifferentiation into smooth muscle-like cells [22] and gut dysmotility in neonatal rodents. *Kit* mutations in animal models result in a decreased number of gut ICC and gut dysmotility [23–26]. *Kit* mutations have also been reported to be associated with other gastrointestinal problems, including neoplasia of the stomach and gastric ulcer [27–31]. In this study we investigated the effect of BM transplantation on gastrointestinal motility and ICC in Kit-hypomorphic W/W^v mice that have reduced ICC populations and gastrointestinal dysmotilities. We demonstrate that transplanted BM-derived cells may have the potential to restore gut dysmotility by differentiating into ICCs.

Methods

Experimental animals and reagents

The W and W^v mutant alleles contain a truncation of the transmembrane domain and point mutation of the kinase domain of Kit, respectively [32]. W/W^v mice were generated as the F1 offspring of WB-W/+ female and C57BL/6-W^v/+ male mice at Japan SLC Inc. (Hamamatsu, Shizuoka, Japan). GFP^+ mice with wild-type *Kit* (+/+) and the same genetic background as W/W^v were produced from WB-+/+ female (Japan SLC) and green fluorescent protein (GFP) transgenic male mice [GFP-Tg mice; C57BL/6 TgN(β-act-EGFP)Osb], which were kindly provided by Professor Masaru Okabe (Genome Information Research Center, Osaka University, Suita, Osaka, Japan) [33]. Mice were properly anesthetized for sacrifice or BM transplantation with pentobarbital sodium or sevoflurane (Maruishi Pharmaceuticals, Osaka, Japan). All animal studies were reviewed and approved by the Osaka University Institutional Committee on the Use and Care of Animals.

Reagents were purchased from Cosmo Bio (Tokyo, Japan), or Nacalai Tesque (Kyoto, Japan), unless stated otherwise.

Preparation of murine BM cells

Bone marrow-derived cell transplantation was performed using female W/W^v mice as recipients and male W/W^v and syngeneic GFP^+ +/+ mice as donors. For BM cell isolation, male W/W^v mice or GFP^+ +/+ mice (6 weeks old) were killed by an anesthetic overdose, and their limbs were removed. BM cells were obtained by flushing the medullary cavities of the tibias and femurs with BM medium (Medium 199, Invitrogen, San Diego, CA) supplemented with 10% fetal bovine serum (FBS; PAA Laboratories GmbH, Pasching, Austria) and 1% antibiotics and antimycotics (Invitrogen, San Diego, CA) using a 26-G needle. BM cells were then sieved through 50-μm meshes, hemolyzed by incubation in ACK buffer (0.15 M NH_4Cl, 1 mM $KHCO_3$, and 0.1 mM EDTA-Na_2, pH 7.2), and washed twice with Medium 199 with 10% FBS and 1% antibiotics and antimycotics.

Cell transplantation

Female W/W^v mice were lethally irradiated (8.5 Gy) using an X-ray generator and intravenously transplanted with BM-derived cells (4×10^6) within 3 h of irradiation.

Four weeks later, blood and spleen samples were obtained and confirmed for GFP chimerism using a flow cytometer (FACS Calibur; BD Biosciences, San Jose, CA) and a fluorescence microscope, respectively.

Assessment of gut motility

Whole gut transit time and gastric emptying were measured 5 and 6 weeks after BM transplantation, respectively. The whole gut transit time was measured according to the method validated by Nagakura et al. [34]. Briefly, mice were administered 2.5% Evans blue in a 1.5% methylcellulose solution (0.3 ml per animal) intragastrically through a stainless steel cannula. Mice were returned to their individual cages, which were placed on a white sheet so that stool colored by the marker could be detected. The time elapsed between the gavage and the appearance of the

marker in the stool was taken as the measure of whole-gut transit.

For measurement of gastric emptying, 0.05% phenol red in 1.5% methylcellulose solution was given intragastrically. Twenty minutes later, the animals were killed and laparotomized with a midline incision. Three additional mice killed immediately after the intragastric administration of the solution served as controls. The cardia and the pylorus were ligated, and the entire stomach was excised and homogenized in 10 ml of 0.1 N NaOH. The phenol red content of the homogenate was measured by spectrophotometry, and gastric emptying was calculated according to the method described by Mashimo et al. [35].

Immunohistochemistry

Whole-mounts

Bone marrow-derived cells were identified by GFP fluorescence or with the aid of anti-GFP antibodies. ICCs were detected with anti-Kit antibodies. The mice were killed, and the jejunum was excised and fixed in acetone on ice for 5 min. Thereafter, the tissues were opened along the mesentery, and washed. The mucosa and submucosa were removed as previously reported [36]. The remaining tissues were blocked with 3% non-immunized goat serum for 1 h then incubated with ACK2, a rat monoclonal anti-Kit antibody (CHEMICON International, Inc., Temecula, CA) and a rabbit polyclonal antibody against GFP (Santa Cruz Biotechnology, Santa Cruz, CA) at 4°C for 2 days. After two 30-min washes in PBS, the tissues were incubated with Cy3-conjugated, affinity-purified goat anti-rat IgG (Jackson Immunoresearch Laboratories Inc., West Grove, PA) and FITC-conjugated goat anti-rabbit IgG antibodies (Santa Cruz Biotechnology) at room temperature for 30 min.

Frozen sections

In these experiments we were unable to use ACK2 for the immunostaining of ICC because detection of cytoplasmic GFP required paraformaldehyde fixation, and ACK2 does not perform well in paraformaldehyde-fixed specimens. Therefore, ICCs were detected with AIC antibody (a generous gift from Professor Shigeko Torihashi; Department of Physical Therapy, Nagoya University School of Medicine, Nagoya, Japan), which withstands paraformaldehyde fixation [37]. This antibody was raised against intact murine ICC purified by immunomagnetic sorting. In wild-type mice, AIC^+ cells have been shown to label Kit^+ ICC [37].

The animals were anesthetized and killed 6 weeks after BM transplantation. The mice were transcardially perfused with PBS and PBS containing 4% paraformaldehyde to flush out blood cells, and the gut was fixed in 4% paraformaldehyde/PBS on ice for 3 h. The specimens were dehydrated through a graded series of sucrose washes (12, 15, and 18%) for 24 h, embedded in Tissue-Tek OCT compound (Sakura Finechemical Co., Tokyo, Japan), and frozen in liquid nitrogen. Cryostat sections (5 μm thick) were mounted onto glass slides and incubated at 37°C for 1 h in PBS with 3% normal goat serum to reduce non-specific immunostaining. The sections were incubated with the AIC antibody at 4°C for 24 h. After three 5-min washes of PBS, the sections were incubated with Cy3-conjugated affinity-purified goat anti-rat IgG as the secondary antibody. After three 5-min washes in PBS, the sections were stained with 4′, 6-diamino-2-phenylindole (DAPI; Vector Laboratories, Inc. Burlingame, CA) and covered with Vectashield, and the transplanted cells were examined by fluorescence microscopy for GFP. Confocal images were obtained by LSM510 (Carl Zeiss, Oberkochen, Germany) or BZ8000 (Keyence, Osaka, Japan). All images were captured using a digital imaging system. To quantitatively investigate the effect of BM transplantation on ICC cell number in W/W^v mice, the areas of AIC positive cells and AIC^+GFP^+ double-positive cells were calculated by image analysis using NIH image software (NIH, Bethesda, MD).

Transmission electron immunomicroscopy

Pre-embedding staining was applied for electron immunomicroscopic observation. In brief, cryostat sections (20 μm thick) were incubated at 37°C for 30 min in 0.3% H_2O_2 methanol and then incubated in 3% normal goat serum at 37°C for 1 h to prevent non-specific binding of mouse immunoglobulins. Sections were incubated with primary antibody against GFP (Santa Cruz Biotechnology, Santa Cruz, CA) in combination with an avidin-biotin detection system (Vector Laboratories) and visualized using 3,3′-diaminobenzidine (DAB; Vector Laboratories). Increased staining contrast was obtained by post-treatment with 1% osmium tetraoxide in PBS for 30 min at room temperature. The samples were dehydrated in ethanol gradient (70, 80, 90, 95, 100, 100, and 100%) and re-embedded in Epon 812. The sections (100 nm thick) were stained with lead and examined under a transmission electron microscope (H-7650, Hitachi High-Technologies, Corporation, Tokyo, Japan).

Statistical analysis

Data shown are mean ± SD. Student's *t* test was used for statistical comparison (StatView ver. 4.51; SAS, Cary, NC). $P < 0.05$ was considered statistically significant.

Results

Restoration of normal gastrointestinal motility by BM transplantation in *W/W^v* mice

W/W^v mice have a partial deficiency of Kit receptor tyrosine kinase [32] and abnormal gut motility compared to wild-type and *W/+* mice [26]. BMs obtained from Kit +/+ GFP-Tg mice or *W/W^v* mice were transplanted into lethally irradiated *W/W^v* mice. Gastrointestinal motility was investigated by measuring whole gut transit time and gastric emptying. Consistent with previous studies in normal mice [34], whole gut transit time in untreated, Kit +/+ GFP-Tg mice was stable and took 194.2 ± 13.3 min. Gastric emptying of liquids was 40.5 ± 19.0% (% emptied at 20 min after gavage), which is also consistent with the previous reports [35].

Whole gut transit and liquid gastric emptying were considerably delayed in *W/W^v* mice transplanted with *W/W^v* BM (275.8 ± 45.3 min and 17.5 ± 7.6%, respectively). In contrast, transplantation of wild-type BM from Kit +/+ GFP-Tg mice significantly improved both whole gut transit time (to 201.1 ± 38.4 min; $P < 0.01$ vs. *W/W^v* mice transplanted with *W/W^v* BM) and fractional gastric emptying at 20 min (31.9 ± 13.8%; $P < 0.05$ vs. *W/W^v* mice transplanted with *W/W^v* BM) (Fig. 1). These results demonstrate that wild-type Kit +/+ BM can restore gut dysmotility in Kit-deficient mice.

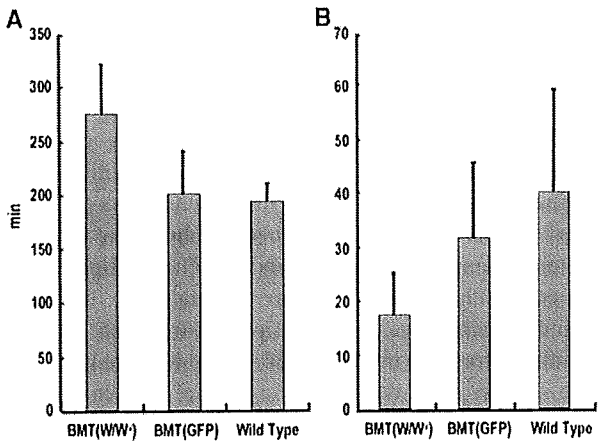

Fig. 1 Whole gut transit time (**a**) and liquid gastric emptying at 20 min (% emptied) (**b**) in *W/W^v* mice transplanted with BM from *W/W^v* mice [BMT(*W/W^v*)] or Kit mice +/+ GFP-Tg mice [BMT(GFP)], and wild-type mice. Five weeks after transplantation, whole-gut transit times were significantly shorter in the mice that had received Kit +/+ GFP-Tg BM than in those that had been transplanted with *W/W^v* BM ($P < 0.01$; $n = 7$ mice per group). Similarly, a significantly greater percentage of the gavaged phenol red solution emptied over the 20-min test period in the mice that had received Kit +/+ GFP-Tg BM ($P < 0.05$; $n = 7$ mice per group). The gastric emptying studies were performed 6 weeks after transplantation

GFP$^+$ BM-derived cells incorporate into ICC networks in *W/W^v* mice

In whole mounts of small intestinal muscle layers of *W/W^v* mice transplanted with Kit +/+ GFP-Tg BM, Kit$^+$ ICC visualized with the aid of ACK2 antibodies were only detected at the level of the deep muscular plexus. Double labeling with anti-GFP antibodies revealed the presence of GFP$^+$Kit$^+$ cells in this layer (Fig. 2). The double-labeled cells were bipolar with their axis oriented along the circumference of the jejunum (Fig. 2). The GFP$^+$Kit$^+$ cells were connected to processes of other Kit$^+$ ICC. No such double-labeled cells were seen in *W/W^v* mice transplanted with *W/W^v* BM.

In cryosections of the stomach, small intestines, and colon, ICC were detected with the aid of AIC, a monoclonal antibody directed against an unidentified cell surface markers of immunomagnetically purified ICC [37]. In these experiments, we visualized GFP-expressing cells by detecting GFP fluorescence. The AIC antibody has been reported to detect ICC in the muscular layers of wild-type mice. It is also reported to stain microvilli, brush border, and some unidentified cells distributed in the mucosa [37]. Consistent with this previous report [37], in our study performed in *W/W^v* mice transplanted with Kit +/+ GFP-Tg BM, AIC labeled some unidentified intramuscular and myenteric cells in the stomach and small intestine, respectively (Fig. 3b, e, respectively). In addition to AIC$^+$ cells, GFP-expressing cells were also detected in unidentified, AIC-negative cells of the muscular, submucosal and mucosal layers of the examined tissues (Fig. 3). However, we only found GFP-expressing AIC$^+$ cells in the myenteric region of the stomach (Fig. 3a–c), in the deep muscular plexus region of the small intestine (Fig. 3d–f), and in the submucosal border of the colon (Fig. 3g–i), which suggests that these cells could be classified as ICCs, because ICCs are reported to be located in these regions of the gastrointestinal tract. As shown in Fig. 4a–c, GFP$^+$ BM transplantation significantly increased AIC$^+$ cells distributed in the region where ICCs were reported to be located compared with *W/W^v* BM transplantation, which indicates that Kit +/+ BM transplantation significantly increased the ICC number in *W/W^v* mice.

Transmission electron immunomicroscopy showed GFP$^+$ cells with abundant mitochondria and rich in endoplasmic reticulum between gut smooth muscle layers, characteristic for gut ICC (Fig. 5).

These results indicate that GFP$^+$ BM cells can incorporate into both ICC and other cells of the gastrointestinal tract of *W/W^v* mice.

Fig. 2 Bone marrow-derived GFP^+ACK2^+ cells (*yellow arrows*) detected in a whole-mount preparation of small intestine. Mucosa and submucosa of the jejunum were removed. The remaining tissues were fixed with acetone and stained with ACK2, a c-Kit antibody and an antibody against GFP. **a** GFP immunofluorescence, **b** Kit immunofluorescence, **c** merged images. *Yellow–orange* color signifies colocalization of GFP and Kit, ×400

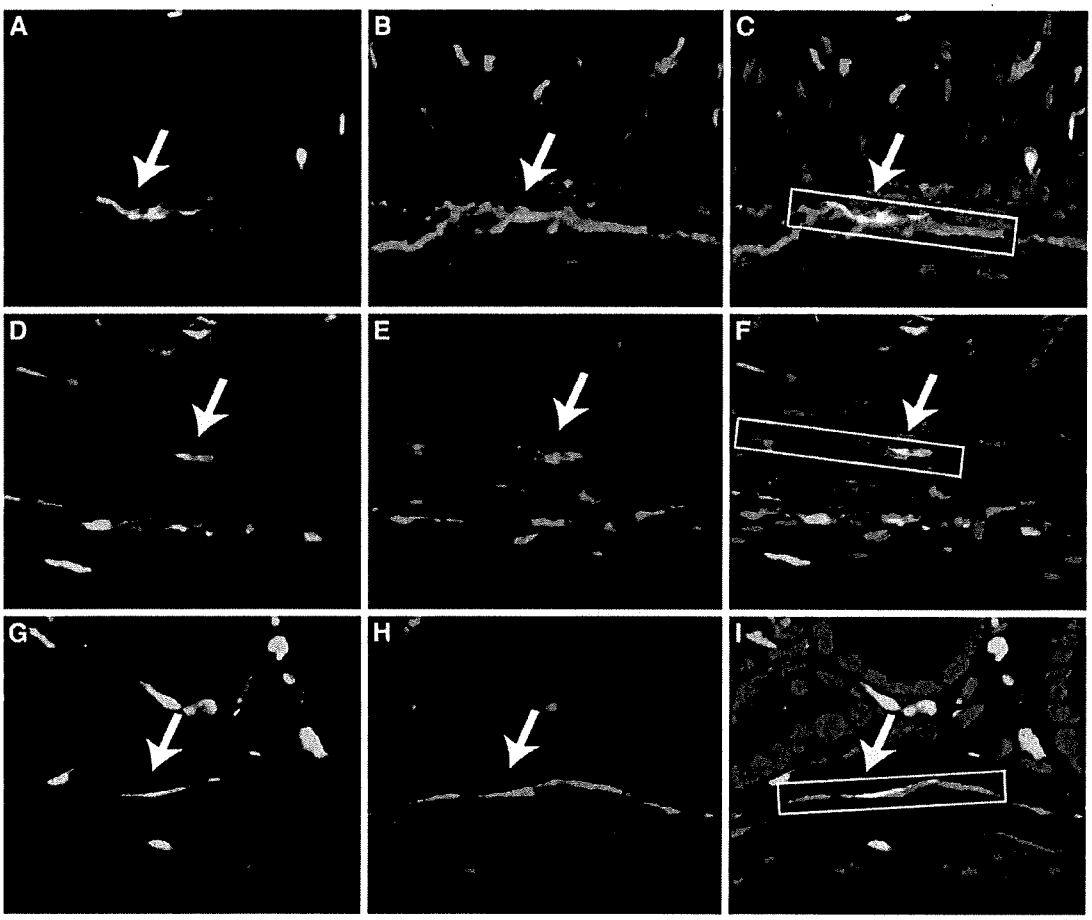

Fig. 3 GFP^+AIC^+ cells detected in stomach (**a–c**), small intestine (**d–f**), and colon (**g–i**) of W/W^v mice transplanted with Kit +/+ GFP-Tg BM. The frozen sections (5 μm thick) were stained with AIC, an antibody against mouse ICC (*red color*; **b**, **e**, **h**). GFP-expressing cells were detected by GFP fluorescence (*green color*; **a**, **d**, **g**). In the merged images (**c**, **f**, **i**), *yellow–orange* color signifies colocalization. *Blue* color in the merged images indicates nuclei visualized with DAPI. GFP-expressing AIC^+ cells are detected only in the myenteric region of the stomach, the deep muscular plexus region of the small intestine, and the submucosal border of the circular muscle layer of the colon, indicated by enclosure in *square* and *yellow arrows*

Discussion

Mutations in *Kit*, the gene encoding for the specific receptor for stem cell factor, cause ICC insufficiency. The complete loss of functional Kit receptor, such as occurs in *W/W* mutants, is lethal. In contrast, the W^v allele, which contains a point mutation in the kinase domain [32], encodes for a partially functioning Kit receptor, so W/W^v

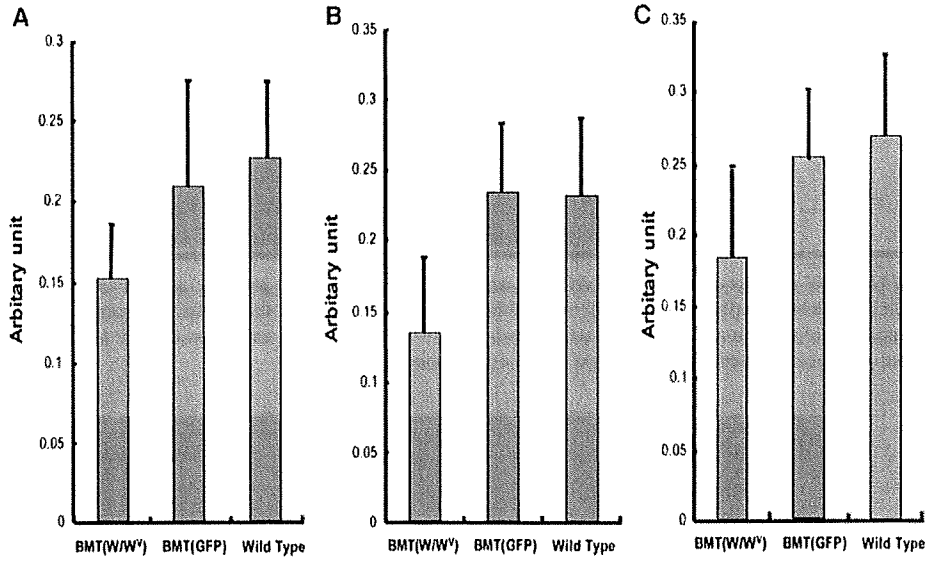

Fig. 4 Quantitative analysis of the effect of BM transplantation on amount of ICC cells in stomach (**a**), small intestine (**b**), and colon (**c**) in *W/W^V* mice transplanted with BM prepared from *W/W^V* mice [BMT(*W/W^V*)] or Kit mice +/+ GFP-Tg mice [BMT(GFP)], and wild-type mice. GFP$^+$ BM transplantation significantly increased AIC$^+$ cells distributed in the region where ICC cells were reported to be located in the mouse gut, compared with *W/W^V* BM transplantation ($P < 0.05$; $n = 4$ mice per group)

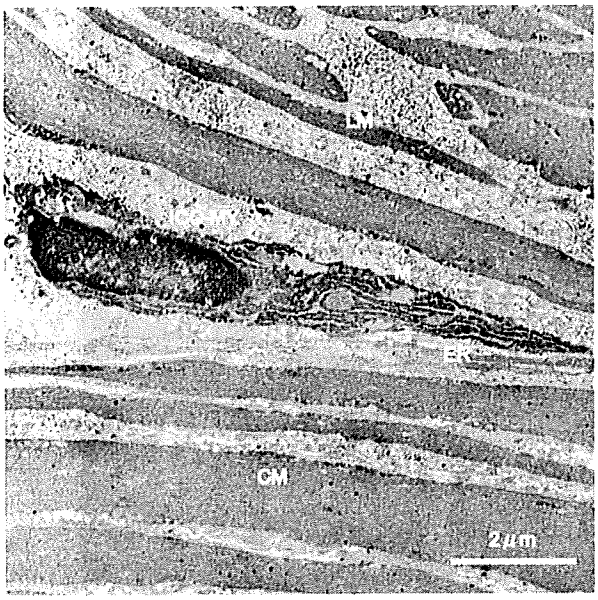

Fig. 5 A transmission electron immunomicroscopic picture demonstrating GFP$^+$ ICC of the colon (*ICC*) between the circular (*CM*) and longitudinal (*LM*) muscle layers. The GFP$^+$ bone marrow-derived cell is identified by dense staining in the cytoplasm and has a spindle shape with mitochondria (*M*) that are wrapped in sheaths of endoplasmic reticulum (*ER*), morphological hallmarks for gut ICC in mice

mice are viable with deficits. For example, ICC populations are reduced in *W/W^V* mice, and these animals have a variety of gut dysmotilities. In the present study we demonstrated that BM transplantation can restore whole gut transit time and gastric emptying in Kit-deficient mice. We also show that BM-derived cells visualized either by detecting GFP fluorescence or with the aid of GFP immunofluorescence can incorporate into ICC networks of the stomach, small intestines, and colon of *W/W^V* mice. The BM-derived, GFP$^+$Kit$^+$ or GFP$^+$AIC$^+$ cells had morphological features of ICC (bipolar or spindle-shaped, and rich in mitochondria and endoplasmic reticulum) and were found in regions normally occupied by ICC. These results suggest that BM cells have the capability of differentiating into ICC or otherwise incorporating into ICC networks of the gastrointestinal tract.

Besides transdifferentiation, cell fusion may also account for the presence of double positive cells in the gastrointestinal tracts of BM-transplanted mice. For example, cell fusion has been shown to be partly responsible for the appearance of GFP$^+$ hepatocytes after BM transplantation into liver-damaged mice [38]. In this study, the possibility of cell fusion was not examined. In the future, the possibility of cell fusion should be investigated using fluorescence in situ hybridization in sex-mismatched BM transplantation.

Deficiency of ICC has been demonstrated in various gastrointestinal motility disorders in humans and animals [1–13, 23–25], including the above-mentioned motor disorders. ICCs direct the electrical rhythmicity and peristalsis of the gut [26, 39]. Furthermore, blocking Kit signaling with a neutralizing antibody [40] or with imatinib mesylate [41, 42], a clinically available receptor tyrosine kinase inhibitor developed for leukemia and gastrointestinal stromal tumors, causes loss of ICC and electrical rhythmicity in mice. These results suggest important roles for maintenance of ICC in gut movement. It follows that patients with severe gut dysmotilities would probably benefit from the restitution of ICCs.

For restoration of ICCs, their origin must be elucidated [43]. It has been suggested that ICC and smooth muscle

cells arise from common mesenchymal precursors in the embryo [44]. Recently, it has been reported that rare $Kit^{low}CD34^{+}CD44^{+}$ cells of the gut muscles may be local ICC precursors [15]. However, those cells are not readily utilizable for therapeutic purposes due to their low numbers and the difficulties in obtaining tissues for harvesting them. BM is easy to obtain and contains stem cells of both mesenchymal lineages, and it may be a good source of ICC precursors as well.

In conclusion, our results suggest that BM-derived cells are potential sources of gut ICC. BM transplantation has a potential to supply adult somatic precursors of ICC in a mouse model of ICC deficiency. Via estimation of ICC function after BM transplantation by measurement of slow wave and determination of cell type in transplanted BM that is responsible for restoration of gastrointestinal motility, the mechanism of BM transplantation to improve motility in ICC dysfunction should be clarified for development of more efficient therapies. Additionally, to open the way to a new therapeutic modality of gut dysmotility, development of instruments and methods for selection, expansion, and implantation of such ICC precursors are required.

Acknowledgments The authors thank Professors Shigeko Torihashi and Masaru Okabe for providing the AIC antibody and the GFP-Tg mice, respectively. Shuji Ishii conducted most of the experiments. Shingo Tsuji was the primary investigator who planned the study. Masahiko Tsujii, Tetsuo Takehara, Sunao Kawano, and Norio Hayashi contributed to the design of the study and interpretation of the results. Tsutomu Nishida performed bone marrow transplantation. Hideki Iijima participated in the flow cytometry. Kenji Watabe participated in histopathological analyses.

The study was supported by a Grant-in-Aid for Scientific Research from the Japan Society for the Promotion of Science (JSPS; no. 18590681).

References

1. Sanders KM, Koh SD, Ward SM. Interstitial cells of Cajal as pacemakers in the gastrointestinal tract. Annu Rev Physiol. 2006;68:307–43.
2. McHale N, Hollywood M, Sergeant G, Thornbury K. Origin of spontaneous rhythmicity in smooth muscle. J Physiol. 2006;570:23–8.
3. Isozaki K, Hirota S, Miyagawa J, Taniguchi M, Shinomura Y, Matsuzawa Y. Deficiency of c-kit+ cells in patients with a myopathic form of chronic idiopathic intestinal pseudo-obstruction. Am J Gastroenterol. 1997;92:332–4.
4. Vanderwinden JM, Rumessen JJ. Interstitial cells of Cajal in human gut and gastrointestinal disease. Microsc Res Tech. 1999;47:344–60.
5. Chen H, Isozaki K, Nakahara M, Kinoshita K, Shinomura Y, Matsuzawa Y, et al. Possible relationship between deficiency of interstitial cells of Cajal and colonic inertia in a patient with colon malfixation. J Gastroenterol. 2002;37:483–4.
6. Kiyohara T, Shinomura Y, Isozaki K, Nakahara M, Tsutsui S, Nishibayashi H, et al. A decreased number of c-kit-expressing cells in a patient with afferent loop syndrome. J Gastroenterol. 2003;38:390–4.
7. Piotrowska AP, Solari V, Puri P. Distribution of interstitial cells of Cajal in the internal anal sphincter of patients with internal anal sphincter achalasia and Hirschsprung disease. Arch Pathol Lab Med. 2003;127:1192–5.
8. Ordog T, Takayama I, Cheung WK, Ward SM, Sanders KM. Remodeling of networks of interstitial cells of Cajal in a murine model of diabetic gastroparesis. Diabetes. 2000;49:1731–9.
9. Nakahara M, Isozaki K, Hirota S, Vanderwinden JM, Takakura R, Kinoshita K, et al. Deficiency of KIT-positive cells in the colon of patients with diabetes mellitus. J Gastroenterol Hepatol. 2002;17:666–70.
10. Forster J, Damjanov I, Lin Z, Sarosiek I, Wetzel P, McCallum RW. Absence of the interstitial cells of Cajal in patients with gastroparesis and correlation with clinical findings. J Gastrointest Surg. 2005;9:102–8.
11. Chang IY, Glasgow NJ, Takayama I, Horiguchi K, Sanders KM, Ward SM. Loss of interstitial cells of Cajal and development of electrical dysfunction in murine small bowel obstruction. J Physiol. 2001;536:555–68.
12. Yanagida H, Yanase H, Sanders KM, Ward SM. Intestinal surgical resection disrupts electrical rhythmicity, neural responses, and interstitial cell networks. Gastroenterology. 2004; 127:1748–59.
13. Faussone-Pellegrini MS, Gay J, Vannucchi MG, Corsani L, Fioramonti J. Alterations of neurokinin receptors and interstitial cells of Cajal during and after jejunal inflammation induced by *Nippostrongylus brasiliensis* in the rat. Neurogastroenterol Motil. 2002;14:83–95.
14. Young HM, Ciampoli D, Southwell BR, Newgreen DF. Origin of interstitial cells of Cajal in the mouse intestine. Dev Biol. 1996;180:97–107.
15. Lorincz A, Redelman D, Horvath VJ, Bardsley MR, Chen H, Ordog T. Progenitors of interstitial cells of cajal in the postnatal murine stomach. Gastroenterology. 2008;134:1083–93.
16. Petersen BE, Bowen WC, Patrene KD, Mars WM, Sullivan AK, Murase N, et al. Bone marrow as a potential source of hepatic oval cells. Science. 1999;284:1168–70.
17. Ferrari G, Cusella-De Angelis G, Coletta M, Paolucci E, Stornaiuolo A, Cossu G, et al. Muscle regeneration by bone marrow-derived myogenic progenitors. Science. 1998;279:1528–30.
18. Zhang S, Jia Z, Ge J, Gong L, Ma Y, Li T, et al. Purified human bone marrow multipotent mesenchymal stem cells regenerate infarcted myocardium in experimental rats. Cell Transplant. 2005;14:787–98.
19. Houghton J, Stoicov C, Nomura S, Rogers AB, Carlson J, Li H, et al. Gastric cancer originating from bone marrow-derived cells. Science. 2004;306:1568–71.
20. Komori M, Tsuji S, Tsujii M, Murata H, Iijima H, Yasumaru M, et al. Involvement of bone marrow-derived cells in healing of experimental colitis in rats. Wound Repair Regen. 2005;13:109–18.
21. Komori M, Tsuji S, Tsujii M, Murata H, Iijima H, Yasumaru M, et al. Efficiency of bone marrow-derived cells in regeneration of the stomach after induction of ethanol-induced ulcers in rats. J Gastroenterol. 2005;40:591–9.
22. Torihashi S, Nishi K, Tokutomi Y, Nishi T, Ward S, Sanders KM. Blockade of kit signaling induces transdifferentiation of interstitial cells of cajal to a smooth muscle phenotype. Gastroenterology. 1999;117:140–8.
23. Isozaki K, Hirota S, Nakama A, Miyagawa J, Shinomura Y, Xu Z, et al. Disturbed intestinal movement, bile reflux to the stomach, and deficiency of c-kit-expressing cells in Ws/Ws mutant rats. Gastroenterology. 1995;109:456–64.

24. Nakama A, Hirota S, Okazaki T, Nagano K, Kawano S, Hori M, et al. Disturbed pyloric motility in Ws/Ws mutant rats due to deficiency of c-kit-expressing interstitial cells of Cajal. Pathol Int. 1998;48:843–9.
25. Sanders KM, Ordog T, Ward SM. Physiology and pathophysiology of the interstitial cells of Cajal: from bench to bedside. IV. Genetic and animal models of GI motility disorders caused by loss of interstitial cells of Cajal. Am J Physiol Gastrointest Liver Physiol. 2002;282:G747–56.
26. Der-Silaphet T, Malysz J, Hagel S, Larry Arsenault A, Huizinga JD. Interstitial cells of cajal direct normal propulsive contractile activity in the mouse small intestine. Gastroenterology. 1998;114:724–36.
27. Shimada M, Kitamura Y, Yokoyama M, Miyano Y, Maeyama K, Yamatodani A, et al. Spontaneous stomach ulcer in genetically mast-cell depleted W/Wv mice. Nature. 1980;283:662–4.
28. Kitamura Y, Yokoyama M, Matsuda H, Shimada M. Coincidental development of forestomach papilloma and prepyloric ulcer in nontreated mutant mice of W/Wv and SI/SId genotypes. Cancer Res. 1980;40:3392–7.
29. Yokoyama M, Tatsuta M, Baba M, Kitamura Y. Bile reflux: a possible cause of stomach ulcer in nontreated mutant mice of W/WV genotype. Gastroenterology. 1982;82:857–63.
30. Yokoyama M, Kitamura Y, Kohrogi T, Miyoshi I. Necessity of bile for and lack of inhibitory effect of retinoid on development of forestomach papillomas in nontreated mutant mice of the W/Wv genotype. Cancer Res. 1982;42:3806–9.
31. Yokoyama M, Tomoi M, Taguchi T, Nakano T, Asai H, Ono T, et al. Fatal antral ulcer in conventionally fed W/Wv mutant mice given indomethacin by injection. Am J Pathol. 1985;119:367–75.
32. Nocka K, Tan JC, Chiu E, Chu TY, Ray P, Traktman P, et al. Molecular bases of dominant negative and loss of function mutations at the murine c-kit/white spotting locus: W37, Wv, W41 and W. Embo J. 1990;9:1805–13.
33. Okabe M, Ikawa M, Kominami K, Nakanishi T, Nishimune Y. 'Green mice' as a source of ubiquitous green cells. FEBS Lett. 1997;407:313–9.
34. Nagakura Y, Naitoh Y, Kamato T, Yamano M, Miyata K. Compounds possessing 5-HT3 receptor antagonistic activity inhibit intestinal propulsion in mice. Eur J Pharmacol. 1996;311:67–72.
35. Mashimo H, Kjellin A, Goyal RK. Gastric stasis in neuronal nitric oxide synthase-deficient knockout mice. Gastroenterology. 2000;119:766–73.
36. Ordog T, Redelman D, Horvath VJ, Miller LJ, Horowitz B, Sanders KM. Quantitative analysis by flow cytometry of interstitial cells of Cajal, pacemakers, and mediators of neurotransmission in the gastrointestinal tract. Cytometry A. 2004;62:139–49.
37. Torihashi S, Yokoi K, Nagaya H, Aoki K, Fujimoto T. New monoclonal antibody (AIC) identifies interstitial cells of Cajal in the musculature of the mouse gastrointestinal tract. Auton Neurosci. 2004;113:16–23.
38. Vassilopoulos G, Wang PR, Russell DW. Transplanted bone marrow regenerates liver by cell fusion. Nature. 2003;422:901–4.
39. Nakagawa T, Misawa H, Nakajima Y, Takaki M. Absence of peristalsis in the ileum of W/W(V) mutant mice that are selectively deficient in myenteric interstitial cells of Cajal. J Smooth Muscle Res. 2005;41:141–51.
40. Maeda H, Yamagata A, Nishikawa S, Yoshinaga K, Kobayashi S, Nishi K. Requirement of c-kit for development of intestinal pacemaker system. Development. 1992;116:369–75.
41. Beckett EA, Ro S, Bayguinov Y, Sanders KM, Ward SM. Kit signaling is essential for development and maintenance of interstitial cells of Cajal and electrical rhythmicity in the embryonic gastrointestinal tract. Dev Dyn. 2007;236:60–72.
42. Takaki M, Misawa H, Shimizu J, Kuniyasu H, Horiguchi K. Inhibition of gut pacemaker cell formation from mouse ES cells by the c-kit inhibitor. Biochem Biophys Res Commun. 2007;359:354–9.
43. Sanders KM. Interstitial cells of Cajal at the clinical and scientific interface. J Physiol. 2006;576:683–7.
44. Kluppel M, Huizinga JD, Malysz J, Bernstein A. Developmental origin and Kit-dependent development of the interstitial cells of cajal in the mammalian small intestine. Dev Dyn. 1998;211:60–71.

Journal of Viral Hepatitis, 2009 doi:10.1111/j.1365-2893.2009.01182.x

Factors affecting efficacy in patients with genotype 2 chronic hepatitis C treated by pegylated interferon alpha-2b and ribavirin: reducing drug doses has no impact on rapid and sustained virological responses

Y. Inoue,[1] N. Hiramatsu,[1] T. Oze,[1] T. Yakushijin,[1] K. Mochizuki,[1] H. Hagiwara,[2] M. Oshita,[3] E. Mita,[4] H. Fukui,[5] M. Inada,[6] S. Tamura,[7] H. Yoshihara,[8] E. Hayashi,[9] A. Inoue,[10] Y. Imai,[11] M. Kato,[12] T. Miyagi,[1] A. Hohsui,[1] H. Ishida,[1] S. Kiso,[1] T. Kanto,[1] A. Kasahara,[1] T. Takehara[1] and N. Hayashi[1]

[1]*Department of Gastroenterology and Hepatology, Osaka University Graduate School of Medicine, Suita City, Osaka, Japan;* [2]*Kansai Rousai Hospital, Amagasaki, Hyogo, Japan;* [3]*Osaka Police Hospital, Osaka, Osaka, Japan;* [4]*National Hospital Organization Osaka National Hospital, Osaka, Osaka, Japan;* [5]*Yao Municipal Hospital, Yao, Osaka, Japan;* [6]*Toyonaka Municipal Hospital, Toyonaka, Osaka, Japan;* [7]*Minoh City Hospital, Minoh, Osaka, Japan;* [8]*Osaka Rousai Hospital, Sakai, Osaka, Japan;* [9]*Kinki Central Hospital of Mutual Aid Association of Public School Teachers, Itami, Hyogo, Japan;* [10]*Osaka General Medical Center, Osaka, Osaka, Japan;* [11]*Ikeda Municipal Hospital, Ikeda, Osaka, Japan; and* [12]*National Hospital Organization Minami Wakayama Medical Center, Tanabe, Wakayama, Japan*

Received May 2009; accepted for publication June 2009

SUMMARY. Reducing the dose of drug affects treatment efficacy in pegylated interferon (Peg-IFN) and ribavirin combination therapy for patients with hepatitis C virus (HCV) genotype 1. The aim of this study was to investigate the impact of drug exposure, as well as the baseline factors and the virological response on the treatment efficacy for genotype 2 patients. Two-hundred and fifty patients with genotype 2 HCV who were to undergo combination therapy for 24 weeks were included in the study, and 213 completed the treatment. Significantly more patients who achieved a rapid virological response (RVR), defined as HCV RNA negativity at week 4, achieved a sustained virological response (SVR) (92%, 122/133) compared with patients who failed to achieve RVR (48%, 38/80) ($P < 0.0001$). Multivariate logistic-regression analysis showed that only platelet counts [odds ratio (OR), 1.68; confidence interval (CI), 1.002–1.139] and RVR (OR, 11.251; CI, 5.184–24.419) were independently associated with SVR, with no correlation being found for the mean dose of Peg-IFN and ribavirin for RVR and SVR. Furthermore, in the stratification analysis of the timing of viral clearance, neither mean dose of Peg-IFN ($P = 0.795$) nor ribavirin ($P = 0.649$) affected SVR in each group. Among the patients with RVR, the lowest dose group of Peg-IFN (0.77 ± 0.10 μg/kg/week) and ribavirin (6.9 ± 0.90 mg/kg/day) showed 100% and 94% of SVR. Hence, RVR served as an important treatment predictor, and drug exposure had no impact on both SVR and RVR in combination therapy for genotype 2 patients.

Keywords: chronic hepatitis C, drug exposure, genotype 2, peginterferon and ribavirin combination therapy.

INTRODUCTION

The current standard of care for chronic hepatitis C (CHC) patients consists of combination therapy using pegylated interferon (Peg-IFN) and ribavirin [1–3]. Large, randomized clinical trials have demonstrated that 42–52% of hepatitis C virus (HCV) genotype 1 'difficult-to-treat' patients achieved sustained virological response (SVR), whereas 76–84% of HCV genotype 2 or 3 infected patients treated with Peg-IFN and ribavirin achieved SVR [4–6]. It also has been shown that in HCV genotype 2 and 3 infected patients, 24-week treatment regimens are just as effective as 48-week regimens [6,7]. Therefore, current guidelines recommend a 24-week treatment for these patients in contrast to 48 weeks for genotype 1 patients [1–3]. However, as side effects are common and treatment is expensive for this therapy, it would be ideal to be able to further reduce the total amount of drug medication

Abbreviations: ALT, alanine aminotransferase; BMI, body mass index; CHC, chronic hepatitis C; c-EVR, complete early virological response; ETR, end of treatment response; γ-GTP, γ-glutamyl transpeptidase; HCV, hepatitis C virus; IFN, interferon; NPV, negative predictive value; Peg-IFN, pegylated interferon; RVR, rapid virological response; SVR, sustained virological response.

Correspondence: Naoki Hiramatsu, MD, PhD, Department of Gastroenterology and Hepatology, Osaka University Graduate School of Medicine, 2-2 Yamadaoka, Suita City, Osaka 565-0871, Japan. E-mail: hiramatsu@gh.med.osaka-u.ac.jp

without loss of treatment efficacy for genotype 2 and 3 patients.

In HCV genotype 1 patients, reducing drug doses affects treatment efficacy. In our investigation of HCV genotype 1 patients, the rate of complete early virological response (c-EVR), defined as HCV RNA negativity at week 12, was affected by the mean dose of Peg-IFN during the first 12 weeks dose-dependently ($P < 0.0001$) [8]. Furthermore, we showed that only 4% relapse was found in patients given ≥12 mg/kg/day of ribavirin among those with c-EVR, and the relapse rate showed a decline in relation to the increase in the dose of ribavirin ($P = 0.0002$) [9]. On the contrary, it remains to be determined whether treatment efficacy can be preserved by further reducing both drug doses in genotype 2 and 3 patients. Because lower doses are expected to cause fewer adverse effects, it is important to find whether reduced drug doses can be used while retaining efficacy.

In the present study, we retrospectively evaluated the efficacy of Peg-IFN alpha-2b and ribavirin combination therapy for 24 weeks in patients infected with HCV genotype 2 and analysed the factors that affected the treatment efficacy, with particular interests in the drug impact of Peg-IFN and ribavirin.

PATIENTS AND METHODS

Patient selection and study design

Patients considered to be eligible for this study were those infected with HCV genotype 2 who underwent Peg-IFN alpha-2b (Schering-Plough K.K., Tokyo, Japan) and ribavirin (Schering-Plough K.K.) combination therapy from December 2005 to July 2007 at 29 medical institutions taking part in the Osaka Liver Forum and had completed the 24-week observation after a clinical course of 24 weeks. Patients with the following criteria were excluded: hepatitis B virus or human immunodeficiency virus coinfection, decompensated liver disease, severe cardiac, renal, haematological or chronic pulmonary disease, poorly controlled psychiatric disease, poorly controlled diabetes and immunologically mediated disease. Liver biopsy had been performed within 24 months prior to the treatment, and histological results were classified according to the METAVIR scoring system [10].

Written informed consent was obtained from each patient, and the study protocol was reviewed and approved according to the ethical guidelines of the 1975 Declaration of Helsinki by institutional review boards at the respective sites.

Patients were treated with Peg-IFN alpha-2b plus ribavirin for the duration of the study of 24 weeks. Peg-IFN alpha-2b and ribavirin dosages were based on body weight according to the manufacturer's instructions: Peg-IFN alpha-2b was given subcutaneously weekly (45 kg or less, 60 μg/dose; 46–60 kg, 80 μg/dose; 61–75 kg, 100 μg/dose; 76–90 kg, 120 μg/dose; 91 kg or more, 150 μg/dose), and ribavirin was given orally daily (60 kg or less, 600 mg/day; 61–80 kg, 800 mg/day; 81 kg or more, 1000 mg/day). The drug doses were also modified based on the manufacturer's instructions according to the intensity of the haematologic adverse effects.

Virological tests

Serum HCV RNA level was quantified by PCR assay (COBAS Amplicor HCV Test v2.0, Chugai-Roche Diagnostics, Tokyo, Japan), with a sensitivity limit of 5000 IU/mL and a dynamic range from 5000 to 5 000 000 IU/mL [11].

Serum HCV RNA was assessed by qualitative PCR assay (COBAS Amplicor HCV Monitor Test v2.0, Chugai-Roche Diagnostics), with a detection limit of 50 IU/mL [12].

Assessment of efficacy

Serum HCV RNA (qualitatively or quantitatively) was measured at weeks 4, 8, 12 and 24 during treatment and after 24 weeks of follow-up without treatment. Patients were classified as having a rapid virological response (RVR) if serum HCV RNA was undetectable (<50 IU/mL) at week 4 and at the end of treatment response (ETR) at week 24 of treatment. SVR was defined as undetectable HCV RNA at week 24 after treatment. Patients with an ETR who seroreverted to HCV RNA during follow-up were classified as relapsers.

Drug exposure

The amounts of Peg-IFN alpha-2b and ribavirin actually taken by each patient during the treatment period were evaluated by reviewing the medical records. The mean doses of both drugs were calculated individually as averages on the basis of body weight at baseline; Peg-IFN alpha-2b expressed as μg/kg/week and ribavirin as mg/kg/day.

Data collection

The medical records were retrospectively reviewed and the factors necessary for this examination were extracted: age, sex, body weight, body mass index (BMI), basic laboratory assessments, liver histology, quantitative and qualitative HCV RNA, dose of Peg-IFN alpha-2b and ribavirin received at each administration, and the response to treatment.

Statistical analysis

This study was a retrospective study and, for treatment results and the analysis of related factors, analysis was carried out only for cases in which the treatment had been completed (per-protocol analysis). Continuous variables are reported as the mean with standard deviation (SD) or

median level, while categorical variables are shown as the count and proportion. In univariate analysis, the Mann–Whitney *U*-test was used to analyse continuous variables, while chi-squared and Fisher's exact tests were used for analysis of categorical data. Variables with $P < 0.05$ at univariate analysis were retained for the multivariate logistic-regression analysis. Stepwise and multivariate logistic-regression models were used to explore the independent factors that could be used to predict a virological response. The significance of trends in values was determined with the Mantel–Haenszel chi-square test. For all tests, two-sided *P*-values were calculated and the results were considered statistically significant if $P < 0.05$. Statistical analysis was performed using the SPSS program for Windows, version 15.0J (SPSS, Chicago, IL, USA).

RESULTS

The baseline characteristics for the total cohort are shown in Table 1. Most of the patients were female (56%) with a mean age of 54 years. Seventy per cent of the patients were treatment naïve. Of the 250 patients, liver biopsies were performed for 174 patients, and 18 of them had advanced fibrosis (F 3–4).

Of the total of 250 patients, 37 (15%) were withdrawn from treatment because of adverse events: decreased haemoglobin ($n = 10$), psychiatric problems including depression ($n = 9$), fatigue ($n = 3$), thrombocytopenia, neutropenia, pyrexia, rash, cerebral haemorrhage, bleeding of ocular fundus, dyspnea, dizziness, jaundice, transaminase rise, gastrointestinal symptoms ($n = 1$) and other adverse events ($n = 4$). Eight of these patients who discontinued treatment prematurely had SVR (8/37; 22%).

Drug adherence

Seventy-nine of the 213 patients (37%) required dose reduction of Peg-IFN alpha-2b, 99 (46%) of ribavirin because of adverse events (not including patients who later discontinued treatment because of adverse event). Neutropenia (24/79; 30%) and thrombocytopenia (24/79; 30%) were the most common adverse events for dose reduction of Peg-IFN alpha-2b, and decreased haemoglobin (82/99; 83%) for that of ribavirin.

Virological response

Of the 213 patients who completed 24 weeks of treatment and 24 weeks of follow-up, 160 (75%) patients were clear of HCV RNA at week 4, 191 (90%) at week 8, 196 (92%) at week 12. ETR was observed for 195 (92%), and SVR for 160 (75%). The relapse rate was 18% (35/195).

Virological response according to the timing of viral clearance

Positive and negative prediction of sustained virological response according to the timing of viral clearance

We examined SVR rates according to the timing of viral clearance for the case in which HCV RNA was cleared during the treatment (Fig. 1a). The SVR rate was 92% (122/133) for patients clear of HCV RNA until week 4, 64% (37/58) from week 5 until week 8, 20% (1/5) from week 9 until

Table 1 Baseline demographic and viral characteristics of patients

Number of cases	250	
Age (years)*	54.0 ± 12.4	(22–76)
Sex (male/female)	110/140	
Body weight (kg)*	60.3 ± 11.7	(39–99)
Body mass index (kg/m^2)*	23.1 ± 3.2	(16–35)
Past IFN therapy (naïve/experienced)†	175/70	
HCV RNA (KIU/mL)‡	1700	(4–5000 <)
Fibrosis (0/1/2/3/4)§	18/98/40/14/4	
Activity (0/1/2/3)§	15/81/70/8	
White blood cells (/mm^3)*	5210 ± 1,750	(2100–13 870)
Neutrophils (/mm^3)*	2700 ± 1,250	(590–9020)
Red blood cells (×10^4/mm^3)*	436 ± 48	(307–554)
Haemoglobin (g/dL)*	13.9 ± 1.4	(10–18)
Platelets (×10^4/mm^3)*	18.3 ± 6.4	(4–41)
ALT (IU/L)*	79 ± 77	(13–581)
γ-GTP (U/L)*	56 ± 65	(7–479)
Creatinine(mg/dL)*	0.7 ± 0.1	(0.4–1.1)

IFN, interferon; HCV, hepatitis C virus; ALT, alanine aminotransferase; γ-GTP, γ-glutamyl transpeptidase. *Values expressed as mean ± SD (range), †interferon treatment history was not known for five patients, ‡values expressed as median (range), §data for 76 patients are missing.

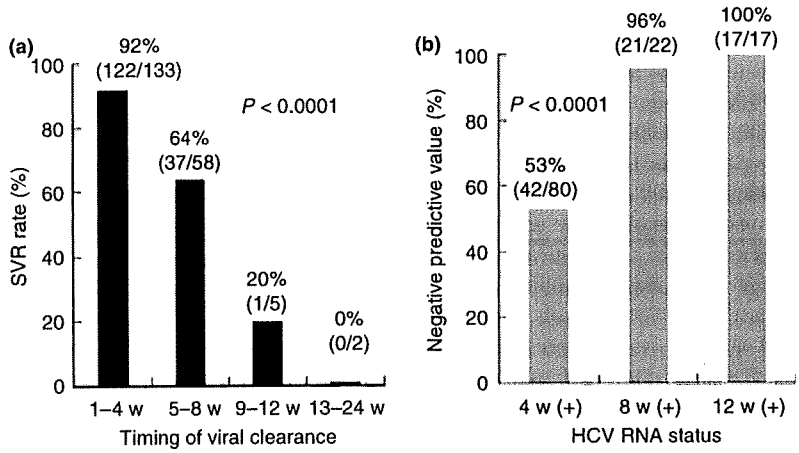

Fig. 1 (a) SVR rates according to timing of viral clearance. The number above each bar shows the percentage, and the numbers inside parentheses show the number of patients showing responses over the total number in the subgroup. The timing of viral clearance was time-dependently correlated with SVR ($P < 0.0001$). (b) Negative predictive values according to time of HCV RNA positivity. The number above each bar shows the percentage, and the numbers inside parentheses show the number of patients showing responses over the total number in the subgroup. The time of HCV RNA positivity was time-dependently correlated with NPV ($P < 0.0001$).

week 12 and 0% (0/2) from week 13 until week 24. The Mantel–Haenszel chi-square test showed that SVR rates were diminished with a delay in the timing of viral clearance becoming late ($P < 0.0001$). Significantly, more patients who attained RVR achieved final SVR (92%, 122/133) than patients who failed to attain RVR (48%, 38/80; $P < 0.0001$).

Next, we examined the negative predictive value (NPV) for the proportion of patients with treatment failure among those with HCV RNA persistence at week 4, 8 and 12 (Fig. 1b). NPV was 53% at week 4, 96% at week 8 and 100% at week 12. Only one of the 22 patients with positive HCV RNA at week 8 reached SVR.

Predictors of sustained virological response

Both pretreatment and treatment factors that could be associated with the response to Peg-IFN and ribavirin combination therapy were compared between patients with and without SVR in Table 2. This univariate analysis showed that age ($P = 0.029$), baseline HCV RNA level ($P = 0.033$), past IFN treatment history ($P = 0.028$), platelets counts ($P = 0.020$) and having RVR ($P < 0.0001$) contributed to achievement of SVR. Factors that were significantly associated with SVR by univariate analysis were then analysed by multivariate logistic regression analysis. SVR was attained independent of high platelet counts [odds ratio (OR) 1.070, 95% confidence interval (CI) 1.003–1.140, $P = 0.040$] and having RVR (OR 11.526, 95% CI 5.317–24.984, $P < 0.0001$; Table 3). As for drug doses, the mean dose of Peg-IFN alpha-2b was 1.32 ± 0.27 μg/kg/week in patients with SVR and 1.27 ± 0.29 μg/kg/week in those without SVR ($P = 0.130$), while that of ribavirin was 10.2 ± 1.9 and 10.2 ± 2.0 mg/kg/day ($P = 0.949$), respectively. Thus, neither Peg-IFN nor ribavirin drug exposure during the full treatment period affected attainment of SVR.

Predictors of rapid virological response

To delineate features that might help identify patients most likely to reach RVR, we also analysed these factors because having RVR turned out to be one of the most powerful predictors of SVR attainment. By univariate and multivariate logistic-regression analyses, RVR was attained independent of younger age (OR 0.648, 95% CI 0.494–0.850, $P = 0.002$) and lower baseline HCV RNA level (OR 0.964, 95% CI 0.944–0.984, $P < 0.0001$; Tables 4 & 5). The mean dose of Peg-IFN alpha-2b during the first 4 weeks was 1.31 ± 0.27 μg/kg/week in patients with RVR and 1.31 ± 0.29 μg/kg/week in those without RVR ($P = 0.259$), that of ribavirin was 10.1 ± 1.8 mg/kg/day and 10.3 ± 2.1 mg/kg/day ($P = 0.637$), respectively. Thus, neither Peg-IFN nor ribavirin drug exposure during the first 4 weeks had an impact on attainment of RVR.

Virological response according to drug exposure and the timing of viral clearance

Impact of drug exposure on sustained virological response

To more closely evaluate the impact of drug exposure on virological response, we classified the average doses of both drugs into four categories (Peg-IFN alpha-2b: up to 0.9 μg/kg/week, from 0.9 to >1.2 μg/kg/week, from 1.2 to >1.5 μg/kg/week, from 1.5 μg/kg/week; ribavirin: up to

Table 2 Factors associated with SVR among patients who completed the treatment – univariate analysis

Factor	SVR (n = 160)	Non-SVR (n = 53)	P-value
Age (years)*	52.4 ± 12.6	56.9 ± 10.2	0.029
Sex (male/female)	66 / 94	26 / 27	0.202
Body weight (kg)*	59.5 ± 11.5	59.9 ± 12.5	0.896
Body mass index (kg/m^2)*	22.8 ± 3.1	22.8 ± 3.5	0.817
HCV RNA (KIU/mL)†	1170	1600	0.033
Past IFN therapy (naive/experienced)‡	116/41	31/22	0.028
Fibrosis (F 0–2/3–4)§	106/10	30/5	0.247
Activity (A 0–1/2–3)§	62/54	20/15	0.847
White blood cells (/mm^3)*	5260 ± 1680	4720 ± 1500	0.078
Neutrophils (/mm^3)*	2740 ± 1270	2420 ± 1020	0.186
Red blood cells (×10^4/mm^3)*	435 ± 44	437 ± 55	0.820
Haemoglobin (g/dL)*	13.9 ± 1.3	14.0 ± 1.5	0.441
Platelets (×10^4/mm^3)*	19.0 ± 6.0	16.5 ± 6.2	0.020
ALT (IU/L)*	86 ± 89	64 ± 45	0.514
γ-GTP (U/L)*	54 ± 67	58 ± 59	0.512
Creatinine (mg/dL)*	0.7 ± 0.1	0.7 ± 0.1	0.457
Mean Peg-IFN dose (μg/kg/week)*	1.32 ± 0.27	1.27 ± 0.29	0.130
Mean ribavirin dose (mg/kg/day)*	10.2 ± 1.9	10.2 ± 2.0	0.949
RVR (yes/no)	122/11	38/42	<0.0001

IFN, interferon; HCV, hepatitis C virus; ALT, alanine aminotransferase; γ-GTP, γ-glutamyl transpeptidase; CI, confidence interval. *Values expressed as mean ± sd, †values expressed as median, ‡interferon treatment history was not known for three patients, §data for 62 patients are missing.

Table 3 Factors associated with SVR among patients who completed the treatment – multivariate analysis

Factor	Category	Odds ratio	95% CI	P-value
Age (years)	By 10	–	–	NS
HCV RNA (KIU/mL)	By 100 KIU/mL	–	–	NS
Platelets (×10^4/mm^3)	By 1 × 10^4/mm^3	1.068	1.002–1.139	0.045
Past IFN therapy	Naïve/experienced	–	–	NS
RVR	Yes/no	11.251	5.184–24.419	<0.0001

IFN, interferon; HCV, hepatitis C virus; CI, confidence interval.

8 mg/kg/day, from 8 to >10 mg/kg/day, from 10 to >12 mg/kg/day, from 12 mg/kg/day). SVR rates relative to the mean drug doses during the full treatment period and the timing of HCV RNA clearance are shown in Table 6. As also shown in Fig. 1a, the respective rates for SVR according to the timing of viral clearance were 92% in patients clear of HCV RNA until week 4, 64% from week 5 until week 8 and 14% from week 9 until week 24. On the contrary, according to mean drug doses, the respective rates for SVR were 89% (24/27), 73% (11/15), 79% (85/107) and 82% (40/49) in patients who received Peg-IFN up to 0.9 μg/kg/week, from 0.9 to >1.2 μg/kg/week, from 1.2 to >1.5 μg/kg/week and from 1.5 μg/kg/week, respectively, and 80% (24/30), 80% (40/50), 82% (68/83) and 79% (27/34) in patients who received ribavirin up to 8 mg/kg/day, from 8 to >10 mg/kg/day, from 10 to >12 mg/kg/day and from 12 mg/kg/day, respectively. If the category of the timing of viral clearance was the same, the respective rates for SVR attainment according to the mean doses of both Peg-IFN and ribavirin were similar. Furthermore, multivariate analysis by the Mantel–Haenszel chi-square test showed that neither the mean dose of Peg-IFN (P = 0.795) nor ribavirin (P = 0.649) affected SVR rates after stratification of the timing of viral clearance. Among the patients with RVR, SVR rates were as high as 88–100% regardless of Peg-IFN alpha-2b medication, and the least medicated group (<0.9 μg/kg/week, the mean dose with SD was 0.77 ± 0.10 μg/kg/week, 0.50–0.89) showed 100% of SVR rate (19/19). Similarly, SVR rates were as high as 91–94% regardless of ribavirin medication among the patients with RVR, and 17 of 18 patients (94%) in the least medicated group (<8 mg/kg/day, the mean dose with SD was 6.9 ± 0.90 mg/kg/day, 5.0–7.9)

Table 4 Factors associated with RVR among patients who completed the treatment – univariate analysis

Factor	RVR (n = 133)	Non-RVR (n = 80)	P-value
Age (years)*	51.9 ± 12.3	56.3 ± 11.3	0.010
Sex (male/female)	60/73	32/48	0.279
Body weight (kg)*	60.2 ± 11.6	58.6 ± 11.9	0.276
Body mass index (kg/m^2)*	22.9 ± 3.2	22.6 ± 3.1	0.369
HCV RNA (KIU/mL)†	1050	1800	0.001
Past IFN therapy (naive/experienced)‡	97/34	50/29	0.068
Fibrosis (F 0–2/3–4)§	86/8	50/7	0.315
Activity (A 0–1/2–3)§	51/43	31/26	1.000
White blood cells (per mm^3)*	5300 ± 1760	4850 ± 1400	0.205
Neutrophils (per mm^3)*	2740 ± 1290	2530 ± 1090	0.340
Red blood cells (×10^4/mm^3)*	440 ± 45	432 ± 49	0.628
Haemoglobin (g/dL)*	13.9 ± 1.4	13.9 ± 1.4	0.975
Platelets (×10^4/mm^3)*	18.9 ± 6.1	17.5 ± 6.1	0.170
ALT (IU/L)*	87 ± 93	69 ± 52	0.630
γ-GTP (U/L)*	57 ± 71	53 ± 53	0.658
Creatinine (mg/dL)*	0.7 ± 0.1	0.7 ± 0.1	0.203
Mean Peg-IFN dose (μg/kg/week)*	1.31 ± 0.27	1.31 ± 0.29	0.259
Mean ribavirin dose (mg/kg/day)*	10.1 ± 1.8	10.3 ± 2.1	0.637

IFN, interferon; HCV, hepatitis C virus; ALT, alanine aminotransferase; γ-GTP, γ-glutamyl transpeptidase; CI, confidence interval. *Values expressed as mean ± SD, †values expressed as median, ‡interferon treatment history was not known for three patients, §data for 62 patients are missing.

Table 5 Factors associated with RVR among patients who completed the treatment – multivariate analysis

Factor	Category	Odds ratio	95% CI	P-value
Age (years)	By 10	0.648	0.494–0.850	0.002
HCV RNA (KIU/mL)	By 100 KIU/mL	0.964	0.944–0.984	<0.0001

HCV, hepatitis C virus; CI, confidence interval.

achieved SVR. In addition, we examined the drug impact on SVR in the patients with the least medication of both drugs (<0.9 μg/kg/week of Peg-IFN and <8 mg/kg/day of ribavirin). Nine patients were categorized into this group and six of these patients achieved SVR (67%); patients with RVR had a significantly higher SVR rate (100%, 5/5) than patients without RVR (25%, 1/4; P = 0.048). Thus, SVR attainment was dependent on time, not on drug dose.

DISCUSSION

In the present study, we found that having RVR and high platelet counts were statistically associated with reaching SVR according to multivariate analysis. The timing of viral clearance was closely related to the treatment effect in patients with genotype 2, similar to the case for those with genotype 1. Ninety-two per cent of SVR was observed for patients with RVR and, conversely, 96% of the patients with HCV RNA positivity at week 8 showed non-SVR. The predictability of SVR based on EVR, defined as a decline of at least 2-log from the baseline of the HCV RNA level at week 12, has been assessed, and genotype 1 patients who have failed to reach EVR are recommended to discontinue the treatment after 12 weeks, because the likelihood of SVR is 0–3% in the absence of EVR [5,13]. On the basis of our examination of patients with genotype 2, not EVR, but 8-week monitoring of the HCV RNA level can be used.

As a significant factor for SVR, not liver fibrosis, but the platelet count was selected. Everson *et al.* [14] reported that patients with low platelet counts (≤12.5 × 10^4/mm^3) achieved lower SVR rates than patients with normal platelet counts (>12.5 × 10^4/mm^3) even in the case of patients with the same category of liver fibrosis treated by Peg-IFN plus ribavirin combination therapy. Thus, independent of liver fibrosis, thrombocytopenia itself seems to participate in treatment failure, although the mechanism remains unknown.

Our study also demonstrated that younger age (OR 0.648, 95% CI 0.494–0.850, P = 0.002) and lower HCV RNA level (OR 0.964, 95% CI 0.944–0.984, P < 0.0001) were statistically associated with reaching an RVR. Zeuzem *et al.* [7] previously reported that pretreatment viral load was not

Table 6 SVR rates according to Peg-IFN alpha-2b and ribavirin exposure and the timing of viral clearance among patients with virological response during the treatment

Timing of viral clearance (week)	Peg-IFN dose (μg/kg/week)				Ribavirin dose (mg/kg/day)				Total
	<0.9	0.9–1.2	1.2–1.5	1.5≤	<8	8–10	10–12	12≤	
1–4	100% (19/19)	91% (10/11)	92% (65/71)	88% (28/32)	94% (17/18)	92% (33/36)	91% (51/56)	91% (20/22)	92% (122/133)
5–8	63% (5/8)	33% (1/3)	64% (19/30)	71% (12/17)	58% (7/12)	54% (7/13)	74% (17/23)	60% (6/10)	64% (37/58)
9–24	–	0% (0/1)	17% (1/6)	–	–	0% (0/1)	0% (0/4)	50% (1/2)	14% (1/7)
Total	89% (24/27)	73% (11/15)	79% (85/107)	82% (40/49)	80% (24/30)	80% (40/50)	82% (68/83)	79% (27/34)	81% (160/198)

*P = 0.795 for comparison of the four Peg-IFN groups after stratification of the timing of viral clearance. **P = 0.649 for comparison of the four ribavirin groups after stratification of the timing of viral clearance.

associated with reaching RVR in genotype 2 patients. In contrast, Dalgard *et al.* [15] reported that independent predictors of RVR in genotype 2 or 3 patients were male gender, younger age (≤40 years) and low viral load (≤400/KIU/mL). The influence of viral load on reaching RVR remains controversial in the Peg-IFN and ribavirin combination therapy in genotype 2 patients, but patients with lower viral load seem favoured to reach HCV RNA levels below the detection limit, that is, to attain RVR, if the virological response is the same.

Recently, because of substantial adverse effects and costs associated with this therapy, studies have been carried out to determine the possibility of further reducing the total amount of drug medication without compromising antiviral efficacy in HCV genotype 2 and 3 patients. There seem to be two ways to achieve. One is by shortening the treatment duration, and the other is by decreasing the doses of the treatment drugs. With respect to the former, several studies on genotype 2 patients have been reported. At first, some studies of small numbers of subjects demonstrated that cumulatively analysed genotype 2 and 3 patients had high SVR rates up to 12 to 16 weeks of therapy (82–94%), similar to patients subjected to 24-week therapy (76–95%) [16–19]. However, further prospective investigation of large numbers of subjects revealed that shortening the treatment duration was associated with an increase in the rate of relapse and that significantly higher relapse rates led to lower SVR rates (71–81.1%), even among those with RVR [15,20,21]. The latest study by Mangia *et al.* [22] showed that shortened therapy after RVR was acceptable only for patients who had no signs of advanced liver fibrosis and low BMI. Considering the results of these trials, shortened therapy is regarded as optional treatment for selected patients displaying favourable baseline characteristics. Therefore, shortening treatment duration from 24 weeks should not be generally recommended for patients who are infected genotype 2 or 3 and can tolerate 24-week Peg-IFN and ribavirin combination therapy.

Another attempt to improve the treatment tolerability for genotype 2 or 3 patients has focused on dose reduction of treatment drugs. Weiland *et al.* [23] examined low-dose Peg-IFN alpha-2a (135 μg weekly) with a weight-based standard-dose of ribavirin (11 mg/kg daily) for genotype 2 and 3 patients. They demonstrated that SVR rates of 86% were achieved, which is equal to those in previous representative randomized controlled studies of standard dose Peg-IFN therapy (76–84%) [4–6]. In contrast, Ferenci *et al.* [24] examined the efficacy of standard-dose Peg-IFN alpha-2a (180 μg weekly) with low-dose ribavirin (400 mg daily) in comparison with standard-dose Peg-IFN alpha-2a (180 μg weekly) and ribavirin (800 mg daily) for genotype 2 and 3 patients, and demonstrated that there was no difference between the two treatment groups with respect to SVR rates (64% with 400 mg/day compared with 69% with 800 mg/day) and relapse rates (20% with 400 mg/day compared